Extraction of the electron self-energy from angle-resolved photoemission data: Application to $Bi_2Sr_2CaCu_2O_{8+x}$

M. R. Norman

Materials Sciences Division, Argonne National Laboratory, Argonne, Illinois 60439

H. Ding*

Materials Sciences Division, Argonne National Laboratory, Argonne, Illinois 60439
and Department of Physics, University of Illinois at Chicago, Chicago, Illinois 60607

H. Fretwell

Department of Physics, University of Illinois at Chicago, Chicago, Illinois 60607

M. Randeria

Tata Institute of Fundamental Research, Mumbai 400005, India

J. C. Campuzano

Materials Sciences Division, Argonne National Laboratory, Argonne, Illinois 60439
and Department of Physics, University of Illinois at Chicago, Chicago, Illinois 60607

The self-energy $\Sigma(\mathbf{k}, \omega)$, the fundamental function that describes the effects of many-body interactions on an electron in a solid, is usually difficult to obtain directly from experimental data. In this paper we show that by making certain reasonable assumptions, the self-energy can be directly determined from angle-resolved photoemission data. We demonstrate this method on data for the high-temperature superconductor $Bi_2Sr_2CaCu_2O_{8+x}$ in the normal, superconducting, and pseudogap phases. [S0163-1829(99)13433-7]

I. INTRODUCTION

The propagation of an electron in a many-body system is described by the Green's function, $G(\mathbf{k},\omega)=1/[\omega-\epsilon_{\mathbf{k}}-\Sigma(\mathbf{k},\omega)]$, where $\epsilon_{\mathbf{k}}$ is the bare energy of the electron and the self-energy $\Sigma(\mathbf{k},\omega)$ encapsulates the effects of many-body interactions. A detailed knowledge of $\Sigma(\mathbf{k},\omega)$ is of critical importance in elucidating the microscopic physics of the system. If its $\mathbf{k}$ dependence is not important, one can obtain information about Σ from a probelike tunneling that measures the density of states given by a $\mathbf{k}$ sum of the imaginary part of G. This was exploited to get a very detailed microscopic understanding of strong-coupling electron-phonon superconductors[1] like lead. In general, though, if Σ depends on $\mathbf{k}$, then momentum-averaged probes cannot be used to extract the self-energy.

The only truly $\mathbf{k}$-resolved probe is angle-resolved photoemission (ARPES). Under the assumption that the ''sudden'' approximation applies (that is, one can ignore the interaction of the photohole with the outgoing photoelectron), for quasi-two-dimensional (2D) systems (since the component of the momentum perpendicular to the surface is not conserved in the photoemission process), and assuming only a single initial state (one ''band''), then the photocurrent can be written in the following form:[2,3]

$$I(\mathbf{k},\omega)=C_{\mathbf{k}}\sum_{\delta\mathbf{k}}\int d\omega' A(\mathbf{k}',\omega')f(\omega')R(\omega-\omega')+B, \tag{1}$$

where $C_{\mathbf{k}}$ is an intensity prefactor (proportional to the square of the dipole matrix element between initial and final states), $A=(-1/\pi)\text{Im}\,G$ is the single-particle spectral function, f is the Fermi function, and R a Gaussian energy resolution function (photon monochromator and detector). The sum $\Sigma_{\delta\mathbf{k}}$ is over a small window in $\mathbf{k}$ space due to the finite angular aperture of the detector. B is the background, which contains extrinsic effects, such as inelastic scattering of the photoelectrons (secondaries).

In this paper, we exploit Eq. (1) to determine the electron self-energy, and illustrate this for ARPES data on the high-temperature superconductor $Bi_2Sr_2CaCu_2O_{8+x}$ (Bi2212). In Sec. II, we introduce the methodology that is necessary to extract the self-energy from the data. In Sec. III, we discuss the issue of background subtraction. In Sec. IV, various results are presented for Bi2212 in the normal, superconducting, and pseudogap phases. Finally, some concluding remarks are offered in Sec. V.

II. METHODOLOGY

Let us assume we know A. Given that, we can easily obtain Σ. A Kramers-Kronig transform of A will give us the real part of G,

$$\text{Re}\,G(\omega)=\text{P}\int_{-\infty}^{+\infty}d\omega'\frac{A(\omega')}{\omega'-\omega}, \tag{2}$$

where P denotes the principal part of the integral. Knowing now both $\operatorname{Im} G$ and $\operatorname{Re} G$, then Σ can be directly read off from the definition of G,

$$\operatorname{Im} \Sigma = \frac{\operatorname{Im} G}{(\operatorname{Re} G)^2 + (\operatorname{Im} G)^2},$$

$$\operatorname{Re} \Sigma = \omega - \epsilon - \frac{\operatorname{Re} G}{(\operatorname{Re} G)^2 + (\operatorname{Im} G)^2}. \quad (3)$$

To obtain $\operatorname{Re} G$ using Eq. (2) we need to know A for *all* energies. From ARPES, though, we only know the product of A and f. (While unoccupied states can be studied by inverse photoemission, its resolution at present is too poor to be useful for our purposes.) This is not a limitation if an occupied $\mathbf{k}$ state is being analyzed and one can either ignore the unoccupied weight or use a simple extrapolation for it (except that only $\operatorname{Re} \Sigma + \epsilon$ is determined). On the other hand, one is usually interested in k vectors near the Fermi surface. Therefore a key assumption will have to be made. We can implement our procedure if we make the assumption of particle-hole symmetry, $A(\epsilon_{\mathbf{k}}, \omega) = A(-\epsilon_{\mathbf{k}}, -\omega)$, within the small $\mathbf{k}$ window centered at $\mathbf{k}_F$. Then, A is obtained by exploiting the identity $A(\epsilon_{\mathbf{k}}, \omega) f(\omega) + A(-\epsilon_{\mathbf{k}}, -\omega) f(-\omega) = A(\epsilon_{\mathbf{k}}, \omega)$, which holds even in the presence of the energy resolution integration in Eq. (1). Note, this can only be invoked at $\mathbf{k}_F$, and was used in our past work to remove the Fermi function from ARPES data,[4,5] where it was denoted as the symmetrization procedure (note that the ''symmetrized'' data will correspond to the raw data for $\omega \lesssim -2.2$ kT). Although the particle-hole symmetry assumption is reasonable for small $|\omega|$ where it can be tested in the normal state by seeing whether the ''symmetrized'' spectrum has a maximum at the Fermi energy (E_F), it will almost certainly fail for sufficiently large $\omega > 0$. Nevertheless, since we only expect to derive Σ for $\omega < 0$, then the unoccupied spectral weight will affect the result only in two ways. The first is through the sum rule $\int d\omega A(\omega) = 1$, which must be used to eliminate the intensity prefactor $C_{\mathbf{k}}$ in Eq. (1). From Eq. (3), we see that violation of the sum rule will simply rescale $\operatorname{Im} \Sigma$, but not $\operatorname{Re} \Sigma$ due to the $\omega - \epsilon$ factor. Our normalization, though, is equivalent to assuming $n_{k_F} = 0.5$, and thus does not involve ''symmetrized'' data. The second influence comes from the Kramers-Kronig transformation in Eq. (2), which is a bigger problem. Fortunately, the contribution from large $\omega' > 0$, for which our assumption is least valid, is suppressed by $1/(\omega' - \omega)$. Further, for $\mathbf{k}_F$, $\epsilon_{\mathbf{k}} = 0$, and thus $\operatorname{Re} \Sigma$ is not plagued by an unknown constant.

Some comments should be made about using real data. Data noise is amplified in the Kramers-Kronig transformation in Eq. (2), and it is desirable to filter the data. We have found for our purposes that a wavelet transform works excellently in this regard, in that it provides smoothed data without any distortion of intrinsic spectral features, such as the quasiparticle peak. We employ a ''denoising'' algorithm[6] that transforms the data into the ''wavelet domain'' using class 6 complex Daubechies wavelets.[7] Then, all wavelet components with absolute values below a certain threshold are set to zero and the data are transformed back into the signal domain. The threshold is set at a level that removes all (or most) of the noise from the data. The advantage of using a wavelet transform, over, e.g., a Fourier filter, comes from the localized nature of the wavelets in the signal and wavelet domain, i.e., the removal of noise from one portion of the data has no effect on intrinsic features elsewhere.

Moreover, it is desirable to obtain a self-energy that is not artificially broadened in ω due to energy resolution. This is handled by deconvoluting the energy resolution out of the data using a maximum entropy method[8] based on the ''Cambridge Algorithm''[9] which we have found to be quite stable. Here, the entropy of a distribution is defined to be $S = -\Sigma_n p_n \ln p_n$, where p_n is the intensity at point n. The algorithm locates the solution with maximum entropy, subject to its being consistent with the data when convoluted with the experimental resolution. Consistency testing is done using the χ^2 statistic (C), $C = \Sigma_n (D_n - F_n R)^2 / \sigma_n^2$, where D_n are the data, $F_n R$ is the solution (F_n) convoluted with the resolution function (R), and σ_n^2 is the variance of datum n. Since a completely flat solution has maximum entropy, the algorithm selects the smoothest (''deconvoluted'') solution consistent with the original data and should only generate structures that are demanded by the data, i.e., those which are above the noise. To minimize the effects of the resolution, we use a high-resolution data set ($\sigma = 7.5$ meV, FWHM$=18$ meV) in the low binding energy range, and combine this with a lower-resolution data set ($\sigma = 15$ meV, FWHM$=35$ meV) to extend the spectrum out to higher binding energy (this takes advantage of the fact that sharp spectral structures only appear at low binding energies). The effects of broadening due to the finite momentum window can be minimized by looking at regions of the Brillouin zone where the dispersion is weak, which is the case considered here (our momentum window has a radius $0.045\pi/a$). This will be less of an issue when considering data from the new high-resolution detectors currently becoming available, where the momentum window can be smaller in area by a factor of 25 or more.

III. BACKGROUND SUBTRACTION

We now illustrate our method by using data from the high-temperature superconductor Bi2212. We choose this material because of its obvious interest to the condensed-matter physics community, the electronic phases it exhibits as a function of doping and temperature, its lack of dispersion along the c axis that justifies the 2D approximation implicit in Eq. (1),[10] and our own strong familiarity with its spectra. On the downside, there is the background issue implicit in Eq. (1). Looking at the ARPES spectra over a large binding energy range, we see that the near-E_F spectral features of interest to us ride on top of a large background. Not only is it too large to be ascribed entirely to the incoherent part of the spectral function A, the ratio of the spectral peak to the background changes with photon energy implying that most, if not all of the background, is extrinsic. This is supported by the fact that the magnitude of the background is sensitive to the photon incident angle and polarization. Moreover, for $\mathbf{k}$ vectors where the spectral peak has dispersed through E_F, this background is still present. It is flat in energy and extends all the way to E_F above T_c, but is gapped in the superconducting state. Taking all of the above facts into account, the likely source of the background is

scattering from other k vectors outside the nominal momentum window, probably due to surface roughness and/or the incommensurate nature of the Bi2212 superstructure.

There are a number of potential ways in which to subtract this background. An ideal way if one is along a symmetry axis (seldom the case) is to subtract data from perpendicular photon polarizations so as to recover that part of the signal that obeys the appropriate dipole selection rules. In practice, one is usually limited to subtracting data from two perpendicular k vectors since the polarization is fixed. Moreover, the finite diameter of the momentum window, possible sample alignment errors, and the enhancement of noise due to subtracting two data sets, limit the effectiveness of this method. Another possibility is to subtract data from an unoccupied k vector under the assumption that it is all background. The obvious problem here, besides the above-mentioned amplification of data noise due to subtracting two data sets, is the strong variation of the dipole matrix elements in the Brillouin zone[11] that can also act to modulate the intensity of the background from one k vector to the next.

Because of this, we have instead explored models that capture the essence of the observed background, in particular a step-edge (flat) background and a ''Shirley'' background.[12] The latter is of the form[13]

$$I(\omega) = P(\omega) + c_{Sh} \int_{\omega}^{\infty} d\omega' P(\omega'), \qquad (4)$$

where I is the total intensity and P that due to primary electrons (thus, one solves for P by simple matrix inversion). Although the step-edge background looks like the ARPES intensity seen for unoccupied **k** states (hence its motivation), it has the disadvantage of having three adjustable parameters (its height, and the position and width of its leading edge). Despite the fact that the Shirley background is designed to model secondary emission, an unlikely source of the background,[13,14] it is similar to the step-edge background, has the advantage of only one adjustable parameter, and has been used extensively in previous treatments.[15,13]

To implement the background subtraction, the high-energy tail of the data is fit to a constant plus a Lorentzian, and then c_{Sh} in Eq. (4) is varied such that this constant becomes zero. This results in a smaller background than simply forcing the intensity to be all background beyond some energy. This is done for data up to 0.5 eV where a minimum is seen in the spectrum, since beyond this, the spectrum rises and thus the ''tail'' becomes completely buried under emission associated with the main valence band. For energies beyond 0.5 eV, we assume this Lorentzian tail when performing the integral (to infinity) in Eq. (2) (real, not fitted, data is used below 0.5 eV, of course). The purpose of this procedure is to avoid artificially forcing $\mathrm{Im}\,\Sigma$ to zero at some cutoff (a power-law tail is not used because the resulting integral would not be convergent). Once this background is subtracted, then the data are symmetrized (by adding the data at positive and negative energies), normalized (by invoking the sum rule), then Kramers-Kronig transformed, which is done analytically by assuming A to be linear between data points (the Lorentzian tail beyond 0.5 eV has an analytic transform, of course). A similar procedure is used for the step-edge background. The height of the step is determined
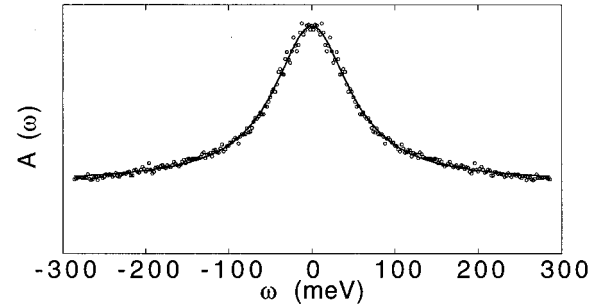

FIG. 1. Symmetrized spectrum for overdoped Bi2212 ($T_c = 72$ K) at $T = 80$ K at the $(\pi,0) - (\pi,\pi)$ Fermi crossing, with the line a fit to a constant plus Lorentzian. For visual purposes, it is shown for $\omega > 0$, though we expect reliable information only for $\omega < 0$. This applies to all the figures.

by fitting the high-energy data to a constant plus a Lorentzian. In the superconducting state, the position and width of the step's leading edge is determined by fitting the low-energy data to a Fermi function (whose ''chemical potential'' is the position and whose ''temperature'' is the width of the step) plus a Gaussian (modeling the spectral peak). In the normal state, the step-edge background simply reverts to a constant in the symmetrized data and so no low-energy modeling is necessary.

IV. RESULTS

In Fig. 1, we show symmetrized data at the $(\pi,0) - (\pi,\pi)$ Fermi crossing for a $T_c = 72$ K overdoped sample at $T = 80$ K, and thus in the normal state. Note that the spectral peak is centered at zero energy, consistent with being at k_F with the zero of energy at E_F. The line is a fit to a Lorentzian plus a constant (flat background), and is an excellent representation of the data [with a half width at half maximum (HWHM) of 55 meV]. This Lorentzian spectral shape at **k** is sufficiently broad to make the quasiparticle ill defined, but may seem unusual given the supposedly expected marginal Fermi-liquid form.[16] We have always found Lorentzian fits to work well in the vicinity of the $(\pi,0)$ point in the normal state.[17] Moreover, in Bi2201, where the normal state can be accessed over a large temperature range, we again find equally good Lorentzian fits even at low temperatures. The difference from optical conductivity data,[18] which do indicate a marginal Fermi-liquid form, may be resolved by noting that the region near $(\pi,0)$ makes little contribution to the in-plane transport due to the flat dispersion. In fact, near the direction $(0,0) - (\pi,\pi)$, a case has been made that a marginal Fermi-liquid line shape can adequately describe the data if a background subtraction similar to what we employ here is done.[15,13] This points to the possibility of a variation of the momentum dependence of Σ along the Fermi surface, which our method can, in principle, explore with the advent of new detectors with improved momentum resolution. Finally, we note that if we restrict away from small energies, a constant plus a power law fits the data as well as a constant plus a Lorentzian. Typically, the (negative) power α is such that $|\alpha| < 1$ (smaller for smaller doping), which would be consistent with a non-Fermi-liquid line shape.[19,20] The advantage of the Lorentzian is that it goes through all the data,
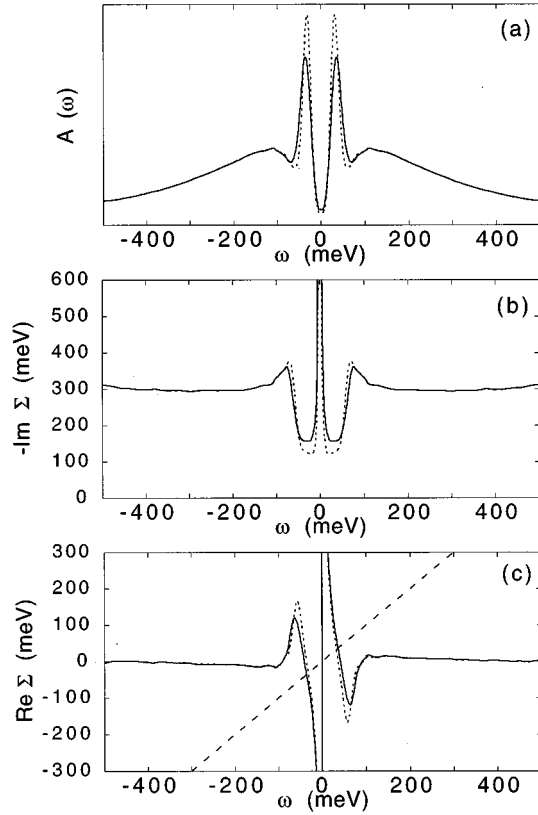
FIG. 2. (a) Symmetrized spectrum (smoothed and Shirley subtracted) for overdoped Bi2212 ($T_c = 87$ K) at $T = 14$ K at (π,0) with (dotted line) and without (solid line) resolution deconvolution. The resulting Im Σ and Re Σ are shown in (b) and (c). The dashed line in (c) determines the condition Re $\Sigma = \omega$.
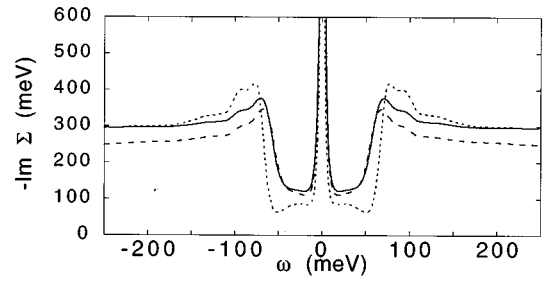

FIG. 3. Im Σ as in Fig. 2(b) (with resolution deconvolution), but for three different background subtractions: Shirley (solid line), step-edge (dotted line), and no subtraction with a cutoff at 0.5 eV (dashed line).

not just the higher-energy part, though this may be fortuitous if part of the ''background'' turns out to be intrinsic (the power-law fit has the potential advantage of a smaller constant background than the Lorentzian fit). A power-law tail would also be divergent in Eq. (2), and thus would have to be cut off (how to do this is not clear, since the tail is buried under the main valence-band emission). This issue will hopefully be resolved in the future by doing a detailed analysis of the spectra as a function of photon energy, photon incident angle, and polarization to determine how much of the ''background'' is truly extrinsic. Once this is achieved, a closer representation of the true self-energy can be obtained.

In Fig. 2(a), we show $T = 14$ K symmetrized data for a $T_c = 87$ K overdoped sample at the (π,0) point (data of Ref. 21). We note the important differences in this superconducting-state spectrum, compared with the normal-state spectrum in Fig. 1, due to the opening of the superconducting gap, with the appearance of a sharp quasiparticle peak displaced from E_F by the superconducting gap, followed by a spectral dip, then by a ''hump'' (Ref. 22) at higher binding energies (where the normal- and superconducting-state spectra coincide[3,21]). This unusual dip-hump structure is only seen near (π,0). The resulting Σ is shown in Figs. 2(b) and 2(c). At high binding energies, one obtains a constant Im Σ as expected from the Lorentzian behavior above T_c in Fig. 1. Note the very large value ($\sim$300 meV), much larger than that implied by Fig. 1 (this is

verified by the normal-state spectrum, which has a much larger HWHM than the normal-state spectrum of Fig. 1). That is, the magnitude of Im Σ strongly increases with reduced doping. Near the spectral dip, Im Σ has a small peak followed by a sharp drop, which we had earlier inferred[21] from the spectral shape guided by fits to the data.[23] This behavior is expected if the electrons are interacting with a spectral distribution gapped by 2Δ in the superconducting state together with a sharp collective-mode inside the 2Δ gap. The current results fully confirm the collective mode explanation proposed in Refs. 21 and 23.

Despite this sharp drop below 70 meV, Im Σ remains quite large at low frequencies. That is, the quasiparticle peak is not resolution limited. Its flat behavior ($\omega^6 \sim \omega^7$) between 20 and 60 meV is consistent with the T^6 dependence of the quasiparticle peak width noted in Ref. 5. Then, below 20 meV, there is a narrow spike in Im Σ. This is the imaginary part of the BCS self-energy, $\Delta^2/(\omega + i0^+)$, which ''kills'' the normal-state pole at $\omega = 0$. The resulting $1/\omega$ divergence of the real part Re Σ, which creates new poles at $\pm\Delta = 32$ meV, is easily seen in Fig. 2(c). This is followed by a strong peak in Re Σ near the spectral dip energy, which follows from the Kramers-Kronig transformation of the sharp drop in Im Σ. The strong peak in Re Σ explains why the low-energy peak in A is so narrow despite the large value of Im Σ. The halfwidth of the spectral peak is given by $\Gamma = $ Im Σ/Z, where $Z = 1 - \partial$ Re $\Sigma/\partial\omega$ (the inverse of the quasiparticle residue). In the vicinity of the spectral peak, Z is large ($\sim$9), giving a Γ of $\sim$14 meV. We note, though, that Γ is still quite sizable, and thus the peak is not resolution limited. As the peak is dispersionless near (π,0),[21] this width is unlikely to be due to momentum resolution, which was verified by simulation. One could ask if it were due to an improper energy resolution deconvolution. This is highly unlikely, which was also checked by simulation. For instance, if one fits the zero-energy spike in Im Σ to a constant plus a Lorentzian, the resulting Lorentzian is extremely narrow (with a HWHM of 2 meV).

It is crucial to understand the extent to which our results for Σ depend upon the choice of various background functions. In Fig. 3, we compare Im Σ [as in Fig. 2(b)] for three different background choices: Shirley, step-edge, and no subtraction at all (for the last case, the spectrum is simply chopped off at 0.5-eV binding energy, and thus no Lorentzian tail). It is reassuring that all three results are qualitatively

similar (at higher binding energies, the unsubtracted case decays to zero because of the cutoff). There are some interesting quantitative differences of the step-edge background from the other two, in particular, the step-like drop in $\mathrm{Im}\,\Sigma$ is more pronounced (resulting in a much more pronounced peak in $\mathrm{Re}\,\Sigma$). This behavior is not very sensitive to the choice of the leading-edge position and width of the step-edge background, and the result is quantitatively close to the theory of Ref. 23. In all cases, $\mathrm{Im}\,\Sigma$ is quite large at low energies, consistent with a quasiparticle peak that is not resolution limited.

We have also looked at data from a $T_c = 85$ K underdoped Bi2212 sample (data of Ref. 4). Below T_c we find behavior quite similar to that of Fig. 2. Of more interest in this case is the so-called pseudogap phase, where a gap is seen in the spectral function above T_c.[24,25] In Fig. 4(a), we show $T = 95$ K symmetrized data at the $(\pi,0)-(\pi,\pi)$ Fermi crossing. One again sees [Fig. 4(b)] a peak in $\mathrm{Im}\,\Sigma$ at $\omega=0$, but it is broadened relative to that of the superconducting state, and the corresponding divergence of $\mathrm{Re}\,\Sigma$ [Fig. 4(c)] is smeared out. Such behavior would be consistent with replacing the BCS self-energy $\Delta^2/(\omega+i0^+)$ by $\Delta^2/(\omega+i\Gamma_0)$. We have recently shown that such a self-energy gives a good description of low-energy data,[5] and can be motivated by considering the presence of pair fluctuations above T_c. In fact, the Σ of Fig. 4 looks remarkably similar to the simple form proposed in Ref. 5, even over a large binding energy range. Note from Fig. 4 that although the equation $\omega-\mathrm{Re}\,\Sigma(\omega)=0$ is still satisfied at $|\omega|\sim\Delta$, $\mathrm{Im}\,\Sigma/Z$ is so large that the spectral peak is strongly broadened in contrast to the sharp peak seen below T_c. Actually, to a good approximation, the spectral function is essentially the inverse of $\mathrm{Im}\,\Sigma$ in the range $|\omega|\lesssim 2\Delta$. We can also contrast this case with data taken above T^*, the temperature at which the pseudogap ''disappears.'' In that case, the spectrum is featureless, and the peak in $\mathrm{Im}\,\Sigma$ is strongly broadened. As the doping increases, this peak in $\mathrm{Im}\,\Sigma$ disappears. Further doping causes a depression in $\mathrm{Im}\,\Sigma$ to develop around $\omega=0$, indicating a crossover to more Fermi-liquidlike behavior.

V. CONCLUSIONS

In conclusion, we have proposed a method for determining the self-energy $\Sigma(\mathbf{k},\omega)$ from ARPES data. Although several important assumptions have to be made (particle-hole symmetry, background subtraction), the method has the advantage that one can directly determine Σ, rather than attempt to guess it by fitting the data.[5,23,26] Given the wealth of information one can obtain, we expect this procedure to be very useful in elucidating the microscopic physics of solids,
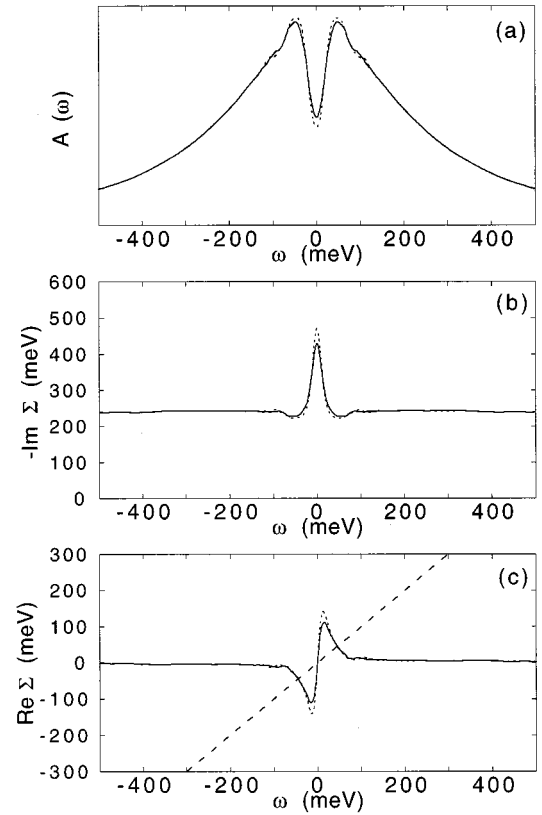

FIG. 4. (a) Symmetrized spectrum (smoothed and Shirley subtracted) for underdoped Bi2212 ($T_c = 85$ K) at $T = 95$ K (pseudogap phase) at the $(\pi,0)-(\pi,\pi)$ Fermi crossing with (dotted line) and without (solid line) resolution deconvolution. The resulting $\mathrm{Im}\,\Sigma$ and $\mathrm{Re}\,\Sigma$ are shown in (b) and (c). The dashed line in (c) determines the condition $\mathrm{Re}\,\Sigma = \omega$.

particularly low-dimensional strongly correlated systems where many controversies exist. Specifically, we find a nontrivial frequency dependence of Σ in the superconducting and pseudogap phases of the high-temperature cuprate superconductors, which puts strong constraints on the microscopic theory for these materials.

*Present address: Department of Physics, Boston College, Chestnut Hill, MA 02467.

[1] J. R. Schrieffer, *Theory of Superconductivity* (Benjamin, New York, 1964).

[2] H. Ding *et al.*, Phys. Rev. Lett. **74**, 2784 (1995).

[3] M. Randeria *et al.*, Phys. Rev. Lett. **74**, 4951 (1995).

[4] M. R. Norman *et al.*, Nature (London) **392**, 157 (1998).

[5] M. R. Norman, M. Randeria, H. Ding, and J. C. Campuzano, Phys. Rev. B **57**, R11 093 (1998).

[6] A. G. Major *et al.*, J. Phys.: Condens. Matter **9**, 10 293 (1997); code supplied by A. G. Major.

[7] I. Daubechies, Commun. Pure Appl. Math. **41**, 909 (1988).

[8] S. B. Dugdale, Ph.D. thesis, University of Bristol, 1996; code supplied by S. B. Dugdale.

[9] J. Skilling and S.F. Gull, in *Maximum Entropy and Bayesian Methods in Inverse Problems*, edited by C. R. Smith and W. T. Grandy, Jr. (Reidel, New York, 1985), p. 83.

[10] H. Ding *et al.*, Phys. Rev. Lett. **76**, 1533 (1996).

[11] A. Bansil and M. Lindroos, J. Phys. Chem. Solids **59**, 1879 (1998).

[12] D. A. Shirley, Phys. Rev. B **5**, 4709 (1972); S. Hufner, *Photoelectron Spectroscopy* (Springer-Verlag, Berlin, 1996).

[13] L. Z. Liu, R. O. Anderson, and J. W. Allen, J. Phys. Chem. Solids **52**, 1473 (1991).

[14] M. R. Norman, M. Randeria, H. Ding, and J. C. Campuzano, Phys. Rev. B **59**, 11 191 (1999).

[15] C. G. Olson *et al.*, Phys. Rev. B **42**, 381 (1990).

[16] C. M. Varma *et al.*, Phys. Rev. Lett. **63**, 1996 (1989).

[17] See also, C. G. Olson *et al.*, Science **245**, 731 (1989).

[18] A. V. Puchkov, D. N. Basov, and T. Timusk, J. Phys.: Condens. Matter **8**, 10 049 (1996).

[19] P. W. Anderson, *The Theory of Superconductivity in the High T_c Cuprates* (Princeton University Press, Princeton, 1997).

[20] S. Misra *et al.*, Phys. Rev. B **58**, 8905 (1998).

[21] M. R. Norman *et al.*, Phys. Rev. Lett. **79**, 3506 (1997).

[22] D. S. Dessau *et al.*, Phys. Rev. Lett. **66**, 2160 (1991).

[23] M. R. Norman and H. Ding, Phys. Rev. B **57**, R11 089 (1998).

[24] H. Ding *et al.*, Nature (London) **382**, 51 (1996).

[25] A. G. Loeser *et al.*, Science **273**, 325 (1996).

[26] R. Claessen *et al.*, Phys. Rev. Lett. **69**, 808 (1992).